ISSN 0016-7932, Geomagnetism and Aeronomy, 2024, Vol. 64, No. 4, pp. 490–499. © Pleiades Publishing, Ltd., 2024.

‘Polar’ Substorms and the Harang Discontinuity

N. G. Kleimenova[a], *, L. I. Gromova[b], S. V. Gromov[b], L. M. Malysheva[a], and I. V. Despirak[c]

[a] *Schmidt Institute Physics of the Earth, Russian Academy of Sciences, Moscow, Russia*

[b] *Pushkov Institute of Terrestrial Magnetism, Ionosphere, and Radio Wave Propagation, Moscow, Troitsk, Russia*

[c] *Polar Geophysical Institute, Apatity, Russia*

**e-mail: ngk1935@yandex.ru*

Received December 13, 2023; revised January 25, 2024; accepted April 4, 2024

Abstract—We analyzed 214 events of ‘polar’ substorms on the Scandinavian meridian IMAGE, i.e., substorms recorded by magnetometers located at geomagnetic latitudes above ~70° MLAT at 1900–0200 MLT during a magnetically quiet time in the absence of negative magnetic bays at lower latitudes. The Harang discontinuity, which separates the westward and eastward electrojets by latitude, is a typical structure for the indicated MLT sector of the high-latitude ionosphere. The global distribution of ionospheric electrojets and the location of the Harang discontinuity during development of ‘polar’ substorms were studied using the maps compiled from the results of spherical harmonic analysis of magnetic measurements on 66 simultaneous ionospheric communications satellites of the AMPERE project. Based on analysis of these maps, it is shown that the instantaneous location of the equatorial boundary of the ionospheric current of a ‘polar’ substorm determines the instantaneous location of the polar boundary of the Harang discontinuity, and the polar boundary of the eastward electrojet determines its equatorial boundary. It has been established that the appearance of 90% of ‘polar’ substorms is observed simultaneously with increasing planetary substorm activity according to the *AL*-index and development of a magnetospheric substorm in the postmidnight sector. At the same time, the development of evening ‘polar’ substorms is associated with the formation of near-midnight magnetic vortices at geomagnetic latitudes of ~70° MLAT (near the “nose” of the Harang discontinuity), indicating a sharp local enhancement of the field-aligned currents. This leads to the formation of a new substorm in the evening sector of near-polar latitudes, called a ‘polar’ substorm with typical features of the onset of a substorm (*Pi*2 geomagnetic pulsation bursts, sudden onset of the substorm close to the equatorial boundary of the contracted oval (the development of a “substorm current wedge”, etc.)

Keywords: magnetoshere, magnetic storm, substorm, ionospheric currents

DOI: 10.1134/S0016793224600310

1. INTRODUCTION

The term ‘substorm,’ introduced by S.-I. Akasofu (1964), means the set of global planetary phenomena observed in the magnetosphere, ionosphere, and on the Earth’s surface arising during the explosive release of energy accumulated in the tail of the magnetosphere due to disturbed solar wind flows around it. One of the main manifestations of a magnetospheric substorm is negative magnetic bays at auroral and subpolar latitudes lasting 1–3 h, e.g., (Rostoker et al., 1980). The development of a substorm is caused by the intensification of large-scale convection, field-aligned currents, and precipitation of auroral particles, e.g., (Baker et al., 1996).

Despite the fact that substorms have been studied quite intensively both experimentally and theoretically, there is still no understanding of where and how substorms arise and begin or what is the mechanism of their excitation. There is not even a clear, generally accepted formulation of the morphological characteristics of a substorm; discussions often arise as to which negative magnetic bay can be called a substorm and which not. There are several contradictory substorm generation models in the literature, and each proposed model is supported by corresponding observational facts. This indicates both the complexity of this phenomenon and the fact that in different geophysical conditions there are different types of magnetospheric substorms with different spatiotemporal dynamics.

Due to the interaction of the solar wind with the Earth’s magnetosphere, plasma convection is constantly observed in the auroral and high-latitude ionosphere, e.g., (Nishida, 1968; Heppner, 1977). Its individual intensifications were called a “convective bay” (Pytte et al., 1978), which is a development of a two-vortex current system *DP2* with vortex centers in the morning (westward electrojet) and evening (eastward electrojet) sectors, as shown in the scheme in Fig. 1a, taken from (Baumjohann, 1983). There are significant differences between a classical magnetospheric substorm and a convective bay (Pytte et al., 1978a; Baumjohann, 1983, Sergeev et al., 2001). Unlike a convec-

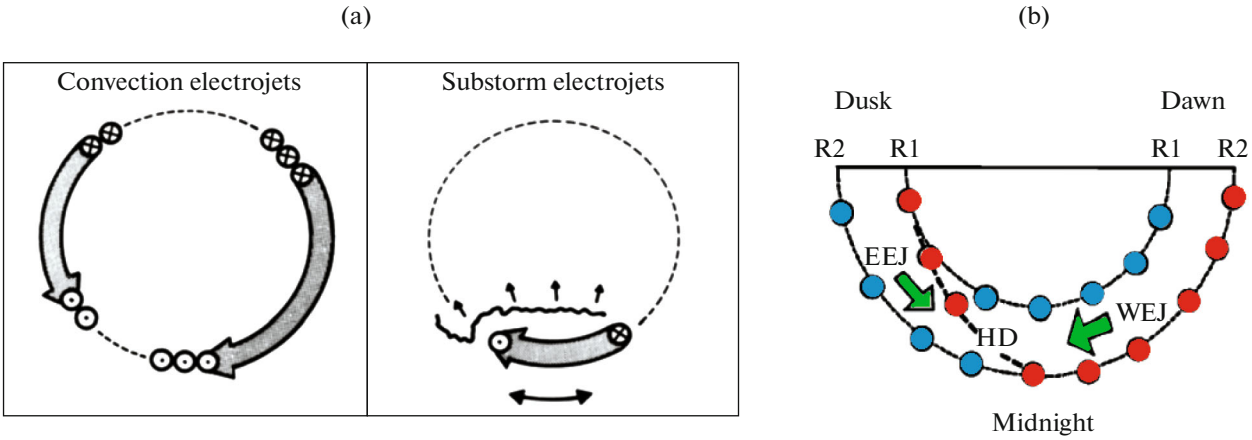

Fig. 1. (a) Scheme of convective bay and magnetospheric substorm from (Baumjohann, 1983); (b) scheme of currents in Harang discontinuity from (Koskinen and Pulkkinen, 1995).

tive bay with a flat, a "classical" substorm is characterized by a sharp onset (substorm onset) with a breakup of auroras, accompanied by the formation of a special 3D system of field-aligned currents forming the so-called "substorm current wedge" (SCW), e.g., (McPherron et al., 1973; Kepko et al., 2015), on the westward edge of which upward field-aligned currents are noted, and on the eastward edge-downward ones. The SCW is a single-vortex current system *DP1* (Fig. 1a). On the earth's surface, the development of a substorm current wedge is accompanied by the appearance of a mid-latitude positive magnetic bay at *X*-component of the field.

A magnetospheric substorm is a typical nighttime disturbance in the region of an auroral oval, which shifts poleward with a decrease in geomagnetic activity (Feldstein and Starkov, 1967). As a rule, a substorm begins with a sudden brightening (breakup) of a calm aurora arc near the equatorial boundary of the auroral oval. Depending on the location of this boundary, the auroral oval is considered "normal" when it is located at 65°–66° MLAT, "expanded", if it is below 65° MLAT, and "contracted", if the equatorial boundary of the oval is above 66°–67° MLAT (Lui et al., 1973). In accordance with this, substorms, depending on the geomagnetic latitude of the location of their onset, are classified as "normal" or "classical," "extended," and substorms "on a contracted oval", which are the least studied and clearly insufficiently.

In recent years, substorms on a contracted oval have been studied in more detail (Kleimenova et al., 2012, 2023; Despirak et al., 2014, 2022; Safargaleev et al., 2018, 2020; Kleimenova et al., 2023), where for brevity such substorms were called 'polar,' since they are observed near the polar edge of the auroral oval. It has been established (Kleimenova et al., 2012, 2023; Kleimenova et al., 2023) that 'polar' substorms are usually recorded at geomagnetic latitudes above ~68°–70° MLAT in the premidnight hours (2000–2200 MLT) under weak geomagnetic activity ($Kp \sim 1-2$) and are accompanied by intense geomagnetic pulsations in the *Pi*2 and *Pi*3 range. Note that according to (Feldstein and Starkov, 1967), the geomagnetic latitude ~68°–70° MLAT corresponds to the equatorial boundary of the evening sector of the auroral oval in magnetically quiet conditions.

Under favorable weather conditions, during 'polar' substorms, high-latitude auroras are recorded as arcs elongated along the oval, sometimes with unusual spiral structures (Safargaleev et al., 2020; Despirak et al., 2022). It was found (Despirak et al., 2014, 2019, 2018) that 'polar' substorms are usually observed during a slow stream of the solar wind, often after the passage of a high-speed recurrent flow. The general patterns of development of 'polar' substorms correspond to the typical characteristics of classical substorms, namely, the formation of a substorm current wedge (positive magnetic bays at lower latitudes), abrupt movement of the electrojet to the pole after the onset of the substorm, and generation of geomagnetic pulsations *Pi*2. Thus, 'polar substorms' can be considered a special type of substorms observed under weakly disturbed conditions in the evening sector of the contracted auroral oval, i.e., at geomagnetic latitudes above ~68°–70° MLAT.

In the region of space typical for the development of 'polar' substorms is the so-called Harang discontinuity (HD) (Harang, 1946; Heppner, 1972; Kamide and Vickrey, 1983), which is a narrow latitudinal band elongated longitudinally in the range ~2100–2400 MLT, separating the westward and eastward electrojets existing simultaneously at different latitudes, i.e., negative (more polar) and positive (more equatorial) magnetic bays (see Kissinger et al., 2013 and references therein). A theoretical explanation for the formation of the Harang discontinuity is given, e.g., in the work by Erickson et al. (1991). The location of the Harang discontinuity and its latitudinal size vary in space and

time depending on geomagnetic conditions, as shown, e.g., in the work by Kunkel et al. (1986).

Figure 1b shows a scheme of the Harang discontinuity for the Northern Hemisphere from (Koskinen and Pulkinen, 1995). In the postmidnight sector, i.e., east of the Harang discontinuity, downward field-aligned currents are located in the higher-latitude (subpolar) zone R1, and upward field-aligned currents are in the more equatorial zone R2, which corresponds to the formation of the westward electrojet of more poleward than the upward field-aligned currents. In the premidnight, evening sector, i.e., west of the Harang discontinuity, the situation is reversed: upward field-aligned currents are observed in high-latitude zone R1, and downward field-aligned currents are observed in lower latitude zone R2, and an eastward electrojet is formed. This means that the Harang discontinuity is characterized by sharp movement of upward field-aligned currents (and the corresponding precipitation of soft electrons) towards the polar boundary of the auroral oval. At the same time, the westward electrojet shifts sharply to the northwest.

A number of studies, e.g., (Nielsen and Greenwald, 1979; Baumjohann et al., 1981; Koskinen and Pulkkinen, 1995; Weygand et al., 2008; Zou et al., 2009), discussed a possible relationship between the onset region of a typical, i.e., classical substorm and the location of the Harang discontinuity. Thus, Nielsen and Greenwald (1979) found that the region of the source of a substorm onset, as a rule, is located slightly more poleward than the Harang discontinuity, determined from ground-based magnetic observations, or it coincides with it. However, other authors (Baumjohann et al., 1981; Koskinen and Pulkkinen, 1995; Bristow et al., 2003; Zou et al., 2009), using radar observations, concluded that the substorm onset source region is more equatorward than the Harang discontinuity by 1°–2° or it coincides with it. This mismatch between the results indicates that the problem of the relationship between the magnetospheric source of substorm onset and the location of the ionospheric Harang discontinuity has not yet been completely resolved; this relationship may be different for different types of magnetic substorms.

The aim of this work is to study the relationship between 'polar' substorms (i.e., substorms on a contracted oval) and the location of the Harang discontinuity.

2. OBSERVATION DATA

The study analyzes ground-based observations on the Scandinavian IMAGE magnetometer network with 10 s sampling (http://space.fmi.fi/image/) (Tanskanen, 2009). Stations of the PPN (Polesie)–NAL (Ny Alesund) profile were used. This is the world's only dense network of stations located almost along the chosen geomagnetic meridian (~100°–110° MLON, with MLT = UT + 2.5 h) from the polar latitudes of Svalbard (NAL ~ 76° MLAT) to mid-latitude stations in Germany (PPN ~ 47° MLAT); the geographic and geomagnetic coordinates of all stations are available on the IMAGE website. On this profile of stations, there is only one "hole" (missing observations), between Svalbard and the continent. The intermediate station between Svalbard and the mainland is Bear Island station (BJN, 71.4° MLAT); the station closest to the continent is Soroya (SOR, 67.8° MLAT). If magnetic bays were observed at BJN but were absent at SOR, then the conditional low-latitude boundary for the occurrence of magnetic bays can be considered the midway between points BJN and NOR, i.e., about 70° MLAT; therefore this latitude was used as the boundary in 'polar' substorm development. This corresponds to the conditions of a contracted oval (Lui et al., 1973). As a rule, the onset of almost all studied 'polar' substorms on the Scandinavian meridional IMAGE profile was observed at BJN observatory or between BJN and SOR. The study also uses data from some mid-latitude stations taken from the website of the INTERMAGNET planetary magnetometer network (https://imag-data.bgs.ac.uk).

The global spatial distribution of ionospheric currents during the studied 'polar' substorms was studied using publicly available data from the AMPERE project, available at http://ampere.jhuapl.edu/products in the form of ionospheric current distribution maps generalized over 10 min, compiled from the results of spherical harmonic analysis of magnetic measurements on 66 simultaneously operating ionospheric satellites at a height of ~780 km. From these measurements, maps of the distribution of field-aligned currents flowing in and out of the ionosphere are also calculated. Unfortunately, these maps are rendered in red and blue, which makes it impossible to present them in the black and white version of the journal, so they are not used here. (Note that color figures are available in the electronic version of the article).

3. OBSERVATION RESULTS

To study the possible relationship between 'polar' substorms and planetary substorm activity, the appearance of 'polar' substorms on the IMAGE meridian was compared with variations in the *AL*-index. We used the same events of 'polar' substorms in winter 2010–2020 (Kleimenova et al., 2023), except for events during which no data on the AMPERE ionospheric satellites were recorded. Thus, 214 events of 'polar' substorms were selected. The research results showed that in 90% of events, the development of 'polar' substorms on the IMAGE profile was accompanied by a simultaneous increase in substorm activity in accordance with the *AL*-index. Analysis of 21 events of 'polar' substorms unaccompanied by a increase of the *AL*-index showed that in 15 events, the westward electrojet in the postmid-

Table 1. Time of 'polar' substorm onset at BJN and substorm at Dikson for four events shown in Fig. 2

Date	Substorm onset at BJN	Substorm onset at DIK
January10, 2012	1900 UT	1855 UT
November 28, 2016	1705 UT	1703 UT
February 13, 2017	1730 UT	1728 UT
January 21, 2018	1900 UT	1856 UT

night sector was observed at very high latitudes, far from the Dikson and Tiksi coastal stations, from which the *AL*-index is calculated. In six events, an increase in the field-aligned current was observed in a very narrow region in terms of longitude and latitude. A similar event was discussed by Despirak et al. (2022).

In addition, the spatial distribution of ionospheric currents was analyzed based on AMPERE satellite observations during the appearance of 'polar' substorms on the IMAGE profile. Studies have shown that before or simultaneously with the onset of the overwhelming majority of evening premidnight 'polar' substorms, an intense magnetic vortex is observed in the near-midnight sector, indicating a sharp local increase in field-aligned currents. A vortex rotating clockwise is an indicator of the intensification of downward field-aligned currents, and a vortex rotating counterclockwise is an indicator of upward field-aligned currents.

Figure 2 shows four examples of AMPERE ionospheric current maps during the onset of typical cases of 'polar' substorms recorded on the IMAGE profile, the location of which is shown by an arrow in the lower left corner of the maps. Graphs of the *AL*-index are also shown below each map at the considered time. All maps show that east of the IMAGE meridian in the early morning sector of the Earth, the development of a westward electrojet is observed at geomagnetic latitudes on the order of 70° MLAT, i.e., above the typical latitudes of classical substorms.

The onset of the 'polar' substorm on the IMAGE meridian can be most clearly determined from observations at BJN. For the events considered in Fig. 2, we compared the data at BJN with observations at Dikson station (DIK, geomagnetic coordinates 157° MLON and 69.3° MLAT; magnetograms are not given in the work), located east of Scandinavia. Note that at another Siberian station, Tiksi (197° MLON, 66.7° MLAT; magnetograms are not shown), located at lower geomagnetic latitudes, the amplitude of deviations during the considered substorms was significantly smaller and no abrupt substorm onset was noted. The table 1 shows the start time of the polar substorm (UT) at BJN and the onset of the 'polar' substorm in Dikson for the four events in Fig. 2.

It can be seen that, within a few minutes, the onset of the 'polar' substorm on the IMAGE meridian coincides with the onset of the substorm at Dikson or slightly lags behind it. West of the magnetic vortex, the electrojet moved westward, towards the polar boundary of the evening auroral oval at geomagnetic latitudes up to about 76°–78° MLAT.

In all examples, a near-midnight magnetic vortex is distinctly seen, and most frequently there is the formation of two, and sometimes more simultaneous vortices: closer to the morning edge there is a clockwise-rotating vortex, and closer to the evening edge, there is a counterclockwise-rotating vortex. The first indicates intensification of downward field-aligned currents, and the second, intensification of upward field-aligned currents, accompanied by an increase in soft electron precipitation, causing auroras. The development of the magnetic vortex sharply "turns" the westward electrojet in the premidnight sector towards the polar boundary of the auroral oval, where an ionospheric electrojet with a low-latitude boundary on the order of ~70° MLAT is formed. At lower latitudes, the eastward electrojet intensifies. The narrow, elongated latitudinal boundary between the westward and eastward electrojets is the Harang discontinuity, a "nose" that starts from the magnetic vortex, extending to the west.

The location of the Harang discontinuity is clearly visible on all four AMPERE maps shown in Fig. 2. The maps show that the equatorial boundary of 'polar' substorms represents the polar boundary of the Harang discontinuity, and the polar boundary of the eastward electrojet located at lower latitudes (in subauroral and sometimes even auroral latitudes) are the equatorial boundary of the Harang discontinuity.

Figure 3 examines in detail one of the typical events of 'polar' substorms on December 5, 2020. IMAGE magnetograms are shown on the left, which show the abrupt onset of the 'polar' substorm around 2010 UT at BJN station (71.4° MLAT), and below at SOR station (67.3° MLAT), a positive magnetic bay has already been detected; they are separated by the sea and the Harang discontinuity, and the distance between stations is about 400 km. At the mid-latitude Borok Observatory (BOX, 114° MLON, 54.4° MLAT), a distinct positive magnetic bay is visible at the *X*-component of the field and a distinct positive bay at the *Y*-component of the field, indicating that the source of this substorm is east of this meridian. Figure 3 also shows a magnetogram of the mid-latitude Irkutsk Observatory (IRT, 179° MLON, 47.8° MLAT) 65° east of Borok. Clearly, a negative bay has been recorded in Irkutsk at the *Y*-component of the field, which means that the

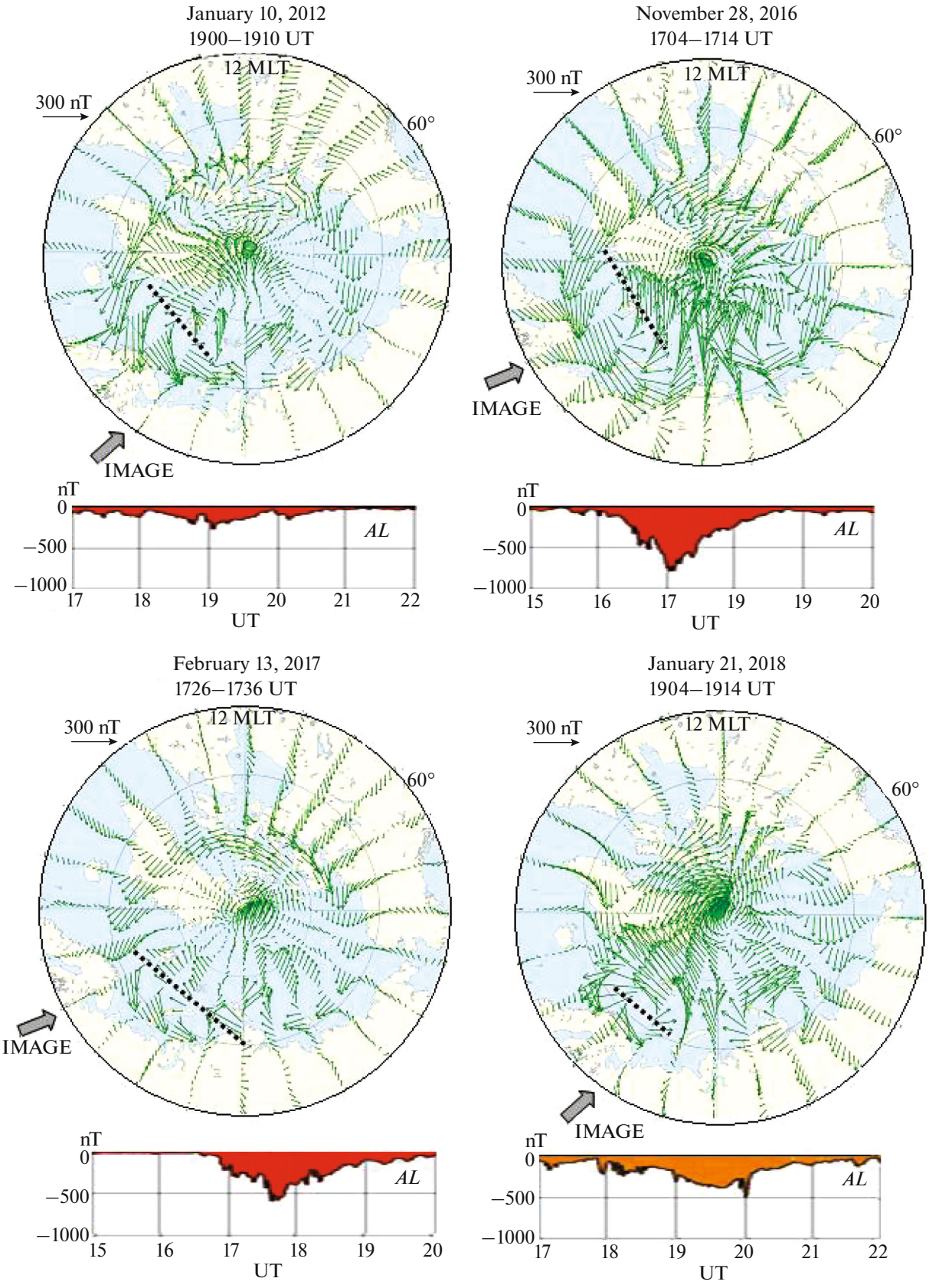

Fig. 2. Typical examples of distribution of global ionospheric currents according to measurements on AMPERE system satellites and variations in planetary substorm *AL*-index during four 'polar' substorms. See text for details.

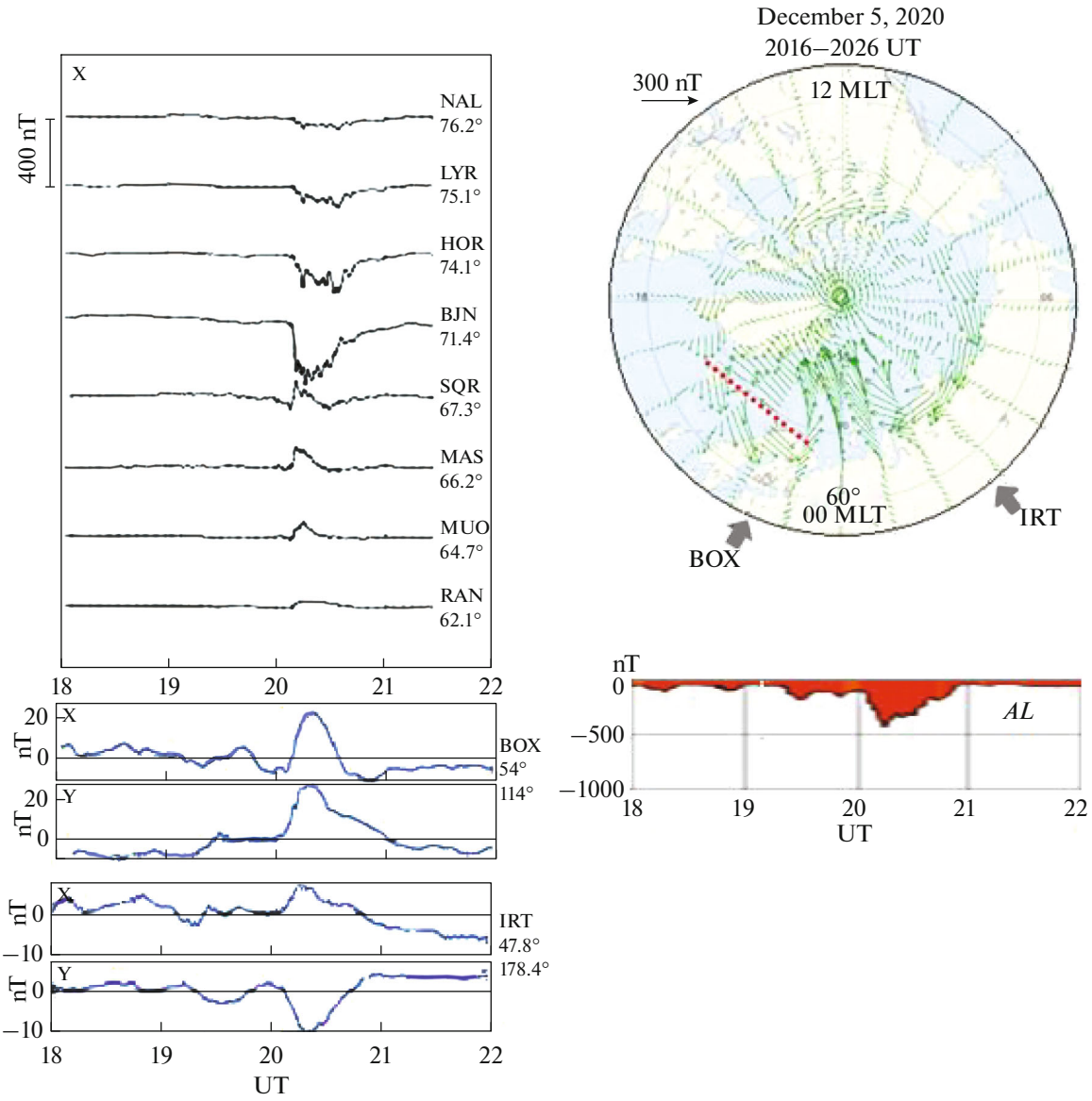

Fig. 3. Example of one typical ‘polar’ substorm on December 5, 2020: magnetograms of some IMAGE stations and mid-latitude Borok (BOX) and Irkutsk (IRT) observatories, as well as map of distribution of ionospheric currents according to AMPERE data and variations in *AL*-index.

source of the substorm is west of Irkutsk, ergo, between Borok and Irkutsk.

This is confirmed by the AMPERE map of the distribution of ionospheric currents shown in the upper right corner, the location of Borok and Irkutsk on which is shown by arrows at the bottom of the map. Three intense magnetic vortices are visible in the near-midnight sector. East of the vortices, the westward electrojet is visible at a latitude of about 70° MLAT, and west of the vortices, the westward electrojet has sharply moved towards the pole; at lower latitudes, the eastward electrojet has intensified. The dotted line on the map shows the Harang discontinuity. The plot of the *AL*-index is shown in the lower right corner of the figure. Clearly, the ‘polar’ substorm on the IMAGE meridian and substorm activity in the nighttime sector begin almost simultaneously (with an accuracy of several minutes).

The source of ‘polar’ substorms observed on the IMAGE network in the subpolar region of the evening sector apparently may be a local increase in field-aligned currents, which is indicated by the development of a magnetic vortex in the near-midnight sector. These magnetic vortices apparently also cause the development of a magnetic substorm east of the vortex, i.e., in the morning sector. Indeed, a number of studies, e.g., (Opgenoorth et al., 1980; Untiedt and Baumjohann, 1993; Lyatsky et al., 2001) have estab-

lished a relationship between the development of a classical substorm and the appearance of a vortex in equivalent ionospheric currents.

4. DISCUSSION

'Polar' substorms are a typical phenomenon in the evening sector of the contracted oval. The concept of a contracted oval means that at the time under discussion, auroras are observed at high latitudes in a narrow region near the polar edge of the auroral oval, i.e., in the same place where we note the appearance of 'polar' substorms. It was previously shown, e.g., (Kleimenova et al., 2012; Despirak et al., 2022), that in favorable weather conditions, 'polar' substorms are usually accompanied by arcs of high-latitude auroras, caused by a local increase in field-aligned currents (therefore, first, 'polar' substorms were studied only in winter periods, when, under favorable weather conditions, observations of auroras were possible). This may confirm that the generation of 'polar' substorms is also associated with an increase in upward field-aligned currents of the R1 zone, which cause auroras. A number of authors believe that the source of these field-aligned currents is located on the flank of the magnetosphere (Ebihara and Tanaka, 2022) and is most likely associated with the low-latitude boundary layer (LLBL) (Bythrow et al., 1981; Siscoe et al., 1991; Troshichev, 2003), where the fast magnetosheath flux can interact with slow magnetospheric fluxes.

Another important question is whether the onset of 'polar' substorms is accompanied by auroral breakup and where the onset source zone is located. Unfortunately, in the vicinity of BJN, where the onset of a 'polar' substorm is usually observed on the IMAGE profile, there are no observations of auroras. However, Milan et al. (2010) present the results of a statistical analysis of the spatiotemporal distribution of more than 2000 auroral breakups (bright flashes of auroras) as an indicator of the onset of a substorm, recorded on the IMAGE satellite. In this study, it was found that at geomagnetic latitudes higher than 67°–68° MLAT, auroral breakups are observed in the premidnight time. This corresponds to the results of a study of 'polar' substorms (Kleimenova et al., 2023). We can conclude that the onset of 'polar' substorms, like classical substorms, is apparently accompanied by the appearance of an auroral breakup, which, unfortunately, due to the lack of ground-based optical observations in the "right" place, has not yet been recorded.

It is known that 10–15 min after the onset of a classical substorm, during the phase of its development, due to the azimuthal pressure of the plasma, auroras and ionospheric currents begin to quickly move to the evening side towards the pole (polar expansion of the substorm), forming a "westward moving traveling surge" (WTS) e.g. (Tighe and Rostoker, 1981; Baumjohann, 1983). It can be suggested that a similar process apparently takes place in weakly disturbed geomagnetic conditions, i.e., with a contracted auroral oval, when the equatorial boundary of the oval is located at sufficiently high geomagnetic latitudes (~68°–70° MLAT), and manifests itself as the development of a special type of substorm in the evening sector, called 'polar' substorms, which, in turn, form the polar boundary of the Harang discontinuity.

Note that in a number of early studies, e.g., (Pytte et al., 1978b; Hones et al., 1985), the appearance of negative magnetic bays at high latitudes was interpreted as the development of a "poleward leap" of a substorm in the late recovery phase of the substorm due to extension of the source field lines far into the tail of the magnetosphere. The same process of stretching field lines into the tail of the magnetosphere explained as the development of a WTS. However, at present, many researchers do not support the "tail" concept of substorm generation and are inclined to think that the source of a substorm is located in a closed magnetosphere. This was even published in a recent study by the "father" of the substorm (Akasofu, 2017).

At the same time, the morphological characteristics of the 'poleward leap' are fundamentally different from the high-latitude expansion of magnetospheric substorms (Pytte et al., 1978), primarily, in the absence of geomagnetic pulsations *Pi*2, as well as the absence of formation of a current wedge (SCW), i.e., the absence of positive magnetic bays at mid-latitudes. Thus, 'polar' substorms can be considered a special type of high-latitude substorms observed in the subpolar latitudes of the evening sector of the contracted auroral oval. 'Polar' substorms form the polar boundary of the Harang discontinuity, and positive magnetic bays observed at lower latitudes form its equatorial boundary.

4. CONCLUSIONS

We have studied the global distribution of the location of ionospheric electrojets and the Harang discontinuity according to satellite measurements of the AMPERE project during 214 'polar' substorms recorded on the Scandinavian meridional profile IMAGE in winter 2010–2020. It has been shown that the instantaneous location of the equatorial boundary of the ionospheric current of the 'polar' substorm determines the instantaneous location of the polar boundary of the Harang discontinuity, and the polar boundary of the eastward electrojet determines its equatorial boundary.

It has been established that 90% of 'polar' substorms are observed simultaneously with an increase in planetary substorm activity according to the *AL*-index and magnetospheric substorm development in the postmidnight sector. In the overwhelming majority of noncoinciding events, the development of the westward electrojet was observed at very high latitudes, significantly higher than the latitudes of the stations from

which *AL*-index of planetary substorm activity is calculated.

It has been shown that the appearance of 'polar' substorms is associated with the development of near-midnight magnetic vortices in the westward ionospheric current, indicating sharp local intensification of field-aligned currents. At the same time, east of the vortex, the ionospheric electrojet of the morning auroral substorm intensifies, and to the west, a sharp shift in the westward ionospheric current to the polar latitudes of the evening sector is observed, similar to the so-called westward travelling surge (WTS), observed after the onset of a classical substorm. This leads to the formation in the evening sector of subpolar latitudes of a new substorm, called a 'polar' substorm with typical characteristic signs of a substorm (bursts in geomagnetic pulsations *Pi*2, substorm onset near the equatorial boundary of the contracted oval at this time, the development of an SCW etc.).

ACKNOWLEDGMENTS

The authors thank the creators of the network databases IMAGE (https://space.fmi.fi/image/), INTERMAGNET (https://imag-data.bgs.ac.uk/GIN_V1/GINForms2), SuperMAG (https://supermag.jhuapl.edu/), and the AMPERE project (http://ampere.jhuapl.edu/products) for the possibility of their use in this study.

FUNDING

The research was carried under the state assignments of the institutes.

CONFLICT OF INTEREST

The authors of this work declare that they have no conflicts of interest.

REFERENCES

Akasofu, S.-I., The development of the auroral substorm, *Planet. Space Sci.*, 1964, vol. 12, no. 4, pp. 273–282. https://doi.org/10.1016/0032-0633(64)90151-5

Akasofu, S.-I., Where is the magnetic energy for the expansion phase of auroral substorms accumulated? 2. The main body, not the magnetotail, *J. Geophys. Res.: Space Phys.*, 2017, vol. 122, pp. 8479–8487. https://doi.org/10.1002/2016JA023074

Baker, D.N., Pulkkinen, T.I., Angelopoulos, V., Baumjohann, W., and McPherron, R.L., Neutral line model of substorms: Past results and present view, *J. Geophys. Res.*, 1996, vol. 101, pp. 12975–13010. https://doi.org/10.1029/95ja03753

Baumjohann, W., Ionospheric and field-aligned current systems in the auroral zone: a concise review, *Adv. Space Res.*, 1983, vol. 2, no. 10, pp. 55–62.

Baumjohann, W., Pellinen, R.J., Opgenoorth, H.J., and Nielsen, E., Joint two-dimensional observations of ground magnetic field and ionospheric electric fields associated with auroral zone currents: current systems associated with local auroral break-ups, *Planet. Space Sci.*, 1981, vol. 29, pp. 431–447. https://doi.org/10.1016/0032-0633(81)90087-8

Bristow, W.A., Sofko, G., Stenbaek-Nielsen, H.C., Wei, S., Lummerzheim, D., and Otto, A., Detailed analysis of substorm observations using SuperDARN, UVI, ground-based magnetometers, and all-sky imagers, *J. Geophys. Res.*, 2003, vol. 108, no. A3, p. 1124. https://doi.org/10.1029/2002JA009242

Bythrow, P.F., Heelis, R.A., Hanson, W.B., Power, R.A., and Hoffman, R.A., Observational evidence for a boundary layer source of dayside region 1 field-aligned currents, *J. Geophys. Res.*, 1981, vol. 86, no. A7, p. 5577. https://doi.org/10.1029/JA086iA07p05577

Despirak, I.V., Lyubchich, A.A., and Kleimenova, N.G., Polar and high latitude substorms and solar wind conditions, *Geomagn. Aeron. (Engl. Transl.)*, 2014, vol. 54, no. 5, pp. 575–582. https://doi.org/10.1134/S0016793214050041

Despirak, I.V., Lubchich, A.A., and Kleimenova, N.G., High-latitude substorm dependence on space weather conditions in solar cycle 23 and 24 (SC23 and SC24), *J. Atmos. Sol.-Terr. Phys.*, 2018, vol. 177, pp. 54–62. https://doi.org/10.1016/j.jastp.2017.09.011

Despirak, I.B., Kleimenova, N.G., Lyubchich, A.A, Malysheva, L.M., Gromova, L.I., Roldugin, A.V., and Kozelov, B.V., Magnetic substorms and auroras at the polar latitudes of Spitsbergen: Events of December 17, 2012, *Bull. Russ. Acad. Sci.: Phys.*, 2022, vol. 86, no. 3, pp. 266–274. https://doi.org/10.3103/S1062873822030091

Ebihara, Y. and Tanaka, T., Where is region 1 field-aligned current generated?, *J. Geophys. Res.: Space Phys.*, 2022, vol. 127, no. 3. https://doi.org/10.1029/2021JA029991

Erickson, G.M., Spiro, R.W., and Wolf, R.A., The physics of the Harang discontinuity, *J. Geophys. Res.*, 1991, vol. 96, pp. 1633–1645. https://doi.org/10.1029/90JA02344

Feldstein, Y.L. and Starkov, G.V., Dynamics of auroral belt and geomagnetic disturbances, *Planet. Space Sci.*, 1967, vol. 15, no. 2, pp. 209–229. https://doi.org/10.1016/0032-0633(67)90190-0

Harang, L., The mean field of disturbance of polar geomagnetic storms, *Terr. Magn. Atmos. Electr.*, 1946, vol. 51, pp. 353–380. https://doi.org/10.1029/TE051i003p00353

Heppner, J.P., The Harang discontinuity in auroral belt ionospheric current, *Geophys. Norv.*, 1972, vol. 29, pp. 105–120.

Heppner, J.P., Empirical models of high-latitude electric fields, *J. Geophys. Res.*, 1977, vol. 82, pp. 1115–1125. https://doi.org/10.1029/JA082i007p01115

Hones, E.W., The poleward leap of the auroral electrojet as seen in auroral images, *J. Geophys. Res.*, 1985, vol. 90, pp. 5333–5337. https://doi.org/10.1029/JA090iA06p05333

Kamide, Y. and Vickrey, J., F. variability of the Harang discontinuity as observed by the Chatanika radar and the IMS Alaska magnetometer chain, *Geophys. Res. Lett.*, 1983, vol. 10, no. 2, pp. 159–162. https://doi.org/10.1029/GL010i002p00159

Kepko, L., McPherron, R.L., Amm, O., et al., Substorm current wedge revisited, *Space Sci. Rev.*, 2015, vol. 190, pp. 1–46. https://doi.org/10.1007/s11214-014-0124-9

Kissinger, J., Wilder, F.D., McPherron, R.L., Hsu, T.-S., Baker, J.B.H., and Kepko, L., Statistical occurrence and dynamics of the Harang discontinuity during steady magnetospheric convection, *J. Geophys. Res.: Space Phys.*, 2013, vol. 118, pp. 5127–5135. https://doi.org/10.1002/jgra.50503

Kleimenova, N.G., Antonova, E.E., Kozyreva, O.V., Malysheva, L.M., Kornilova, T.A., and Kornilov, I.A., Wave structure of magnetic substorms at high latitudes, *Geomagn. Aeron. (Engl. Transl.)*, 2012, vol. 52, no. 6, pp. 746–754. https://doi.org/10.1134/S0016793212060059

Kleimenova N.G., Gromova L.I., Despirak I.B., Malysheva L.M., Gromov S.V., Lyubchich A.A. Features of polar substorms: An analysis of individual events, *Geomagn. Aeron. (Engl. Transl.)*, 2023a, vol. 63, no. 3, pp. 288–299. https://doi.org/10.31857/S0016794023600023

Kleimenova, N.G. and Despirak, I.V., Malysheva, L.M., Gromova, L.I., Lubchich, A.A., Roldugin, A.V., and Gromov, S.V., Substorms on a contracted auroral oval, *J. Atmos. Sol.-Terr. Phys.*, 2023b, vol. 245, pp. 106049–106062. https://doi.org/10.1016/j.jastp.2023.106049

Koskinen, H.E.J. and Pulkkinen, T.I., Midnight velocity shear zone and the concept of Harang discontinuity, *J. Geophys. Res.*, 1995, vol. 100, pp. 9539–9547. https://doi.org/10.1029/95JA00228

Kunkel, T., Baumjohann, W., Untied, J., and Greenwald, R., Electric fields and currents at the Harang discontinuity: A case study, *J. Geophys.*, 1986, vol. 59, pp. 73–86.

Lui, A.T.Y., Perreault, P.D., Akasofu, S.-I., and Anger, C.D., The diffuse aurora, *Planet. Space Sci.*, 1973, vol. 21, no. 5, pp. 857–861. https://doi.org/10.1016/0032-0633(73)90102-5

Lui, A.T.Y., Akasofu, S.-I., Hones, E.W., Jr., Bame, S.J., and McIlwain, C.E., Observation of the plasma sheet during a contracted oval substorm in the prolonged quiet period, *J. Geophys. Res.*, 1976, vol. 81, no. 7, pp. 1415–1419. https://doi.org/10.1029/JA081i007p01415

Lyatsky, W., Cogger, L.L., Jackel, B., Hamza, A.M., Hughes, W.J., Mur, D., and Rasmussen, O., Substorm development as observed by Interball UV imager and 2-D magnetic array, *J. Atmos. Sol.-Terr. Phys.*, 2001, vol. 63, pp. 1609–1621. https://doi.org/10.1016/S1364-6826(01)00045-1

McPherron, R.L., Russell, C.T., and Aubry, M.P., Satellite studies of magnetospheric substorms on August 15, 1968: 9. Phenomenological model for substorms, *J. Geophys. Res.*, 1973, vol. 78, no. 16, pp. 3131–3149. https://doi.org/10.1029/JA078i016p03131

Milan, S.E., Boakes, P.D., and Hubert, B., Response of the expanding/contracting polar cap to weak and strong solar wind driving: implications for substorm onset, *J. Geophys. Res.*, 2008, vol. 113, pp. A09215. https://doi.org/10.1029/2008JA013340

Nielsen, N.E. and Greenwald, A., Electron flow and visual aurora at the Harang discontinuity, *J. Geophys. Res.*, 1979, vol. 84, pp. 4189–4200. https://doi.org/10.1029/JA084iA08p04189

Nishida, A., Geomagnetic DP2 fluctuations and associated magnetospheric phenomena, *J. Geophys. Res.*, 1968, vol. 73, no. 5, pp. 1795–1803. https://doi.org/10.1029/JA073i005p0179

Opgenoorth, H.J., Pellinen, R.J., Maurer, H., Küppers, F., Heikkila, W.J., and Tanskanen, P., Ground-based observations of an onset of localized field-aligned currents during auroral breakup around magnetic midnight, *J. Geophys.*, 1980, vol. 4, pp. 101–115.

Pytte, T., McPherron, R.L., Jr., Hones, E.W., and Wes, H.I., Multiple-satellite studies of magnetospheric substorms, III. Distinction between polar substorms and convection-driven negative bays, *J. Geophys. Res.*, 1978a, vol. 83, no. A2, pp. 663–679.

Pytte, T., McPherron, R.L., Kivelson, M.G., Wes, H.I., Jr., and Hones, E.W., Multiple-satellite studies of magnetospheric substorms: plasma sheet recovery and the poleward leap of auroral zone activity, *J. Geophys. Res.*, 1978b, vol. 83, pp. 5256–5268. https://doi.org/10.1029/JA083iA11p05256

Rostoker, G., Akasofu, S.-I., Foster, J., Greenwald, R.A., Kamide y, Kawasaki, K., Lui, A.T.Y., Mcpherron, R.L., Russell, C.T., Magnetospheric substorms definitions and signatures, *J. Geophys. Res.*, 1980, vol. 85, no. A4, pp. 1663–1668.

Safargaleev, V.V., Mitrofanov, V.M., and Kozlovsky, A.E., Complex analysis of the polar substorm based on magnetic, optical, and radar observations near Spitsbergen, *Geomagn. Aeron. (Engl. Transl.)*, 2018, vol. 58, no. 4, pp. 793–808. https://doi.org/10.1134/S0016793218040151

Safargaleev, V.V., Kozlovsky, A.E., and Mitrofanov, V.M., Polar substorm on 7 December 2015: Preonset phenomena and features of auroral breakup, *Ann. Geophys.*, 2020, vol. 38, no. 4, pp. 901–918. https://doi.org/10.5194/angeo-38-901-2020

Sergeev, V.A., Kubyshkina, M.V., Liou, K., Newell, P.T., Park, G., Nakamura, R., and Mukai, T., Substorm and convection bay compared: Auroral and magnetotail dynamics during convection bay, *J. Geophys. Res.*, 2001, vol. 106, pp. 18843–18855.

Siscoe, G.L., Lotko, W., and Sonnerup, B.U.O., A high-latitude, low-latitude boundary layer model of the convection current system, *J. Geophys. Res.*, 1991, vol. 96, no. A3, p. 3487. https://doi.org/10.1029/90ja02362

Tanskanen, E.F., A comprehensive high-throughput analysis of substorms observed by image magnetometer net-

work: Years 1993–2003 examined, *J. Geophys. Res.*, 2009, vol. 114, p. A05204. https://doi.org/10.1029/2008JA013682

Tighe, W. and Rostoker, G., Characteristics of westward travelling surges during magnetospheric substorms, *J. Geophys.*, 1981, vol. 50, no. 1, pp. 51–67. https://journal.geophysicsjournal.com/JofG/article/view/128.

Troshichev, O.A., Low-latitude boundary layer and generation of field-aligned currents, in *Earth's Low-Latitude Boundary Layer*, Newell, P.T. and Onsager, T., Eds., AGU, 2003, pp. 3329–334. https://doi.org/10.1029/133GM33

Untiedt, J. and Baumjohann, W., Studies of polar current systems using the IMS Scandinavian magnetometer array, *Space Sci. Rev.*, 1993, vol. 63, pp. 245–390. https://doi.org/10.1007/BF00750770

Weygand, J.M., McPherron, R.L., Frey, H., Amm, O., Kauristie, K., Viljanen, A.T., and Koistinen, A., Relation of substorm onset to Harang discontinuity, *J. Geophys. Res.*, 2008, vol. 113, p. A04213. https://doi.org/10.1029/2007JA012537

Zou, S., Lyons, L.R., Wang, C.-P., Boudouridis, A., Ruohoniemi, J.M., and Anderson, P.C., Dyson, P.C., Devlin, J.C., On the coupling between the Harang reversal evolution and substorm dynamics: A synthesis of SuperDARN, DMSP, and IMAGE observations, *J. Geophys. Res.*, 2009, vol. 114, p. A01205. https://doi.org/10.1029/2008JA013449